

**MERCURY'S THIN CRUST** Michael M. Sori, University of Arizona, Tucson, AZ 85721 (sori@lpl.arizona.edu)

**Introduction:** Crustal thickness is a critical parameter for understanding the geological history of a terrestrial planet. At Mercury, data from the MESSENGER spacecraft [1] have allowed for maps of crustal thickness from gravity and topography data [2–5]. The mean crustal thickness was estimated to be  $35 \pm 18$  km by comparing observed admittances at Mercury to those predicted by isostatic models [6]. Similar techniques have also been used to investigate the compensation of topography on other planets [e.g., 7, 8].

The mean crustal thickness value of  $35 \pm 18$  km was calculated assuming that Airy isostasy is achieved when crustal columns of equal area contain equal mass [6]. This assumption is valid in Cartesian geometry, but may represent a state of disequilibrium on a sphere [9, 10], with the magnitude of the discrepancy increasing with decreasing planetary radius [10].

Here, I improve estimates of Mercury's crustal thickness in two ways. First, I calculate crustal grain density to test the hypothesis that Mercury's topography is supported by a Pratt mechanism. This hypothesis is rejected. Second, I use a formulation of Airy isostasy appropriate for spherical geometry that yields a mean crustal thickness of  $26 \pm 11$  km, 25% thinner than previous estimates. I conclude by discussing important geological implications of this new, thin value.

**Grain density and Pratt isostasy:** A Pratt mechanism, in which topography is supported by lateral density variations in the crust, is possible. Under this compensation mechanism, a negative correlation between elevation and density is expected [8, 11]. Ideally, the presence of Pratt isostasy would be tested by searching for such a negative correlation between crustal bulk density and elevation. The gravity field at Mercury is not sufficiently resolved at present to permit a map of the bulk density of the crust. Therefore, I calculate the grain density at the surface.

Previous analysis reported relative chemical abundances of important elements at 205 locations on Mercury's surface [12] using measurements from MESSENGER's X-Ray Spectrometer (XRS) [13]. I use normative mineralogy to convert those relative abundances into a grain density by assuming an absolute Si abundance of 25%, a range of allowable abundances for Fe, and an accounting of S as either elemental S or  $\text{SO}_2$ . For each of these 205 locations, I sample elevation from a MESSENGER-derived topographic map [14].

Results of grain density for the case of an average Fe abundance of 2% and elemental S are shown in Figure 1a. The average grain density is  $3066 \pm 87$   $\text{kg/m}^3$ . Using these results to test Pratt isostasy assumes that the calculated density is representative of the density throughout crustal columns at depth. Be-

cause XRS measurements only sample the upper ~100 microns [13], I exclude data points that represent locations on the surface known to be volcanic or inside large impact basins [15–17]. The remaining 97 data points are exclusively in the intercrater plains and heavily cratered terrain (IcP-HCT), and do not show a statistically significant correlation between density and elevation for any set of assumptions used in the normative mineralogy calculations (e.g., Figure 1b). Therefore, I conclude Pratt isostasy is unlikely to be an important compensation mechanism on Mercury.

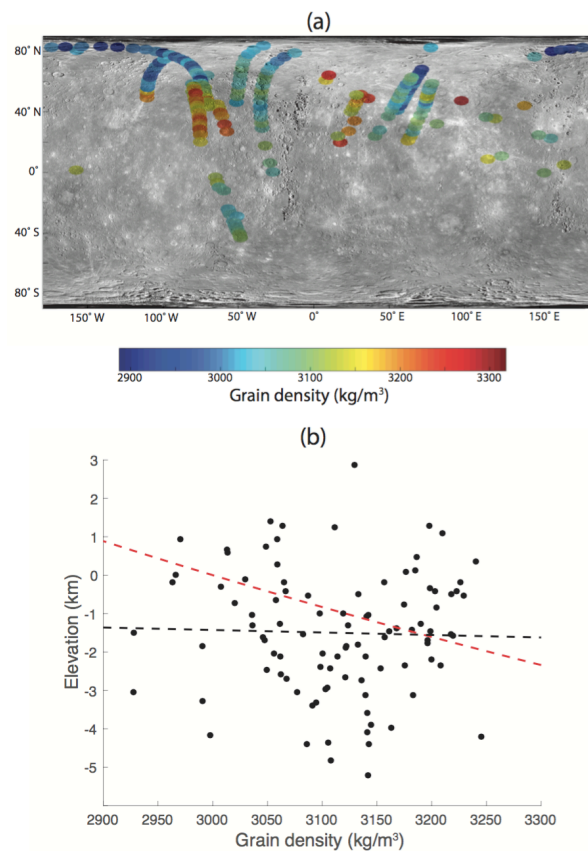


**Figure 1.** (a) Example grain density results overlying a MESSENGER-derived image map of Mercury. (b) Scatter plot of elevation and density measurements for the map in (a). The black dashed line represents the best-fit line between elevation and density; the red dashed line represents the expected relationship from Pratt isostasy.

**Admittance, Airy isostasy, and crustal thickness:**

Previous work calculated the geoid-to-topography ratios (GTRs) in localized regions on Mercury and interpreted a signature of Airy isostasy for certain high-pass filters [6]. This GTR (9 m/km) was then compared to the GTRs predicted by models of Airy isostatic support, which are sums of spectrally-weighted admittanc-

es [14]. The admittances were calculated by defining isostasy as occurring when equal masses were present in crustal columns of equal area.

I calculate admittances under the assumption that isostasy is instead achieved when lateral flow at equipotential surfaces at depth is minimized [9, 10]. This definition is more appropriate when planetary curvature becomes relevant [10]. Admittances in this “equal pressures” case are the same as in the “equal masses” case at high spherical harmonic degrees, but vary at low spherical harmonic degrees. Since admittances are weighted by the fractional topographic power at each spherical harmonic degree [18], and since planetary topography is preferentially greater at low degrees than at high degrees, the predicted GTR for a given isostatic model may be significantly changed in the equal masses vs. equal pressures formulations.

In Figure 2a, I show the predicted admittances for Airy isostasy on Mercury for both formulations. In Figure 2b, I show the resulting GTRs as a function of mean crustal thickness. Both cases assume Airy compensation in a single-layered crust of bulk density  $2900 \text{ kg/m}^3$ , and use the same filter as in the observations [6]. For the observed GTR on Mercury of  $9 \pm 3 \text{ m/km}$  [6], the mean crustal thickness is  $26 \pm 11 \text{ km}$ . As shown in Figure 2c, this value is only weakly dependent upon assumed crustal density.

**Geological implications:** Ideally, one would measure the crustal thickness of Mercury using a combination of a high-degree global gravity field, global topographic data, and seismic analysis. Nonetheless, the currently known gravity and topography data can be analyzed with admittances, yielding a best-fit average crustal thickness of  $26 \pm 11 \text{ km}$ , thinner than any previously published value. This thin value has several important geological implications.

Two implications involve Mercury’s mantle and are informed by lunar studies. First, impact-induced porosity likely extends into the Moon’s mantle [19]; the crustal thickness value here allows for the same phenomenon on Mercury. Second, impact models show the largest impacts on the Moon should have excavated mantle material onto the surface [20]. The Caloris-forming impact was suggested to similarly excavate Mercury’s mantle assuming a crustal thickness of  $50 \text{ km}$  [21]; the new mean crustal thickness value here makes this process almost certain. Attempts to spectroscopically observe the upper mantle, as has been done on the Moon [22], may therefore be possible.

Finally, the mean crustal thickness calculated here implies 7% of Mercury’s silicate material is in its crust. Similarly, lunar crustal volume represents 7% of its silicate material. Mercury and the Moon therefore experienced a similar degree of crustal production; Mercury is not uniquely efficient at crustal production as was previously thought.

**Conclusions:** Mercury’s best-fit mean crustal thickness from MESSENGER data is  $26 \pm 11 \text{ km}$ . This value is thinner than previously published estimates, and has several important implications for the planet’s geological history. This analysis should be repeated when more global data for Mercury is acquired from the future BepiColombo mission [23].

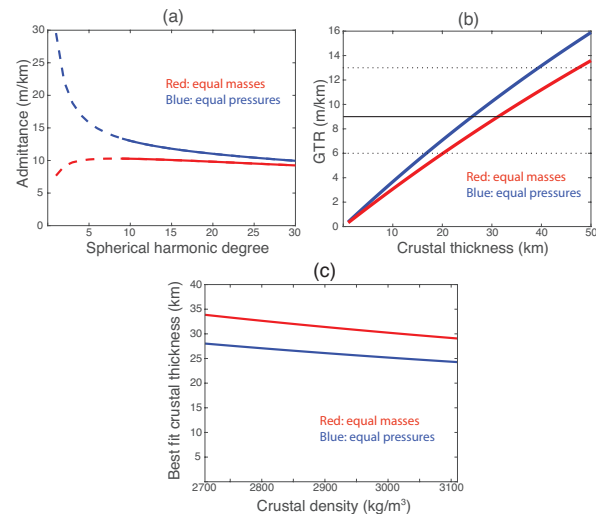


**Figure 2.** Comparison of results for equal mass vs. equal pressure calculations of modeled (a) admittances, (b) GTRs, and (c) crustal thicknesses. The solid and dotted lines in (b) represent the best-fit and bounds on the observed GTR from [6]. The dashed lines in (a) represent the degrees excluded in the filter of [6] to calculate this observed GTR value.

**References:** [1] Solomon, S.C. (2001), *Planet. Space Sci.* 49. [2] Smith, D.E., et al. (2010), *Icarus* 209. [3] Smith, D.E., et al. (2012), *Science* 336. [4] Mazarico, E., et al. (2014), *J. Geophys. Res. Planets* 119. [5] James, P.B., et al. (2015), *J. Geophys. Res. Planets* 120. [6] Padovan, S., et al. (2015), *Geophys. Res. Lett.* 42. [7] James, P.B., M.T. Zuber, and R.J. Phillips (2013), *J. Geophys. Res. Planets* 118. [8] Sori, M.M., et al. (2018), *J. Geophys. Res. Planets*, in revision. [9] Turcotte, D.L., et al. (1981), *J. Geophys. Res.* 86. [10] Hemingway, D.J. and I. Matsuyama (2017), *Geophys. Res. Lett.* 44. [11] Solomon, S.C. (1978), *Proc. LPSC 9<sup>th</sup>*. [12] Weider, S.Z., et al. (2015), *Earth Planet. Sci. Lett.* 416. [13] Nittler, L.R., et al. (2011), *Science* 333. [14] Becker, K.J., et al. (2016), *LPSC 47<sup>th</sup>*. [15] Denevi, B.W., et al. *Science* 324. [16] Head, J.W., et al. (2011), *Science* 333. [17] Ostrach, L.R., et al. (2015), *Icarus* 250. [18] Wieczorek, M.A. and R.J. Phillips (1997), *J. Geophys. Res.* 102. [19] Wieczorek, M.A., et al. (2013), *Science* 339. [20] Miljković, K., et al. (2015), *Earth Planet. Sci. Lett.* 409. [21] Potter, R.W.K. and J.W. Head (2017), *Earth Planet. Sci. Lett.* 474. [22] Melosh, H.J., et al. (2017), *Geology* 45. [23] Benkhoff, J., et al., *Planet. Space Sci.* 58.